

LARGE-EDDY SIMULATION OF AIR FLOW WITHIN A SQUARE ENCLOSURE WITH A PARTIALLY HEATED BOTTOM SURFACE AND COOLED VERTICAL WALLS

Rogério Fernandes Brito

Federal University of Itajuba – UNIFEI – BPS, Av., #1303, Zip Code: 37500-903, Pinheirinho, Itajubá, Brazil.
rogbrito@unifei.edu.br

Paulo Mohallem Guimarães

Federal University of Itajuba – UNIFEI – BPS, Av., #1303, Zip Code: 37500-903, Pinheirinho, Itajubá, Brazil.
paulomgui@uol.com.br

Aristeu da Silveira Neto

Federal University of Uberlandia – UFU – Joao Pinheiro Av., #565, Zip Code: 38400-902, Uberlandia, Brazil.
aristeus@mecanica.ufu.br

Genésio José Menon

Federal University of Itajuba – UNIFEI – BPS, Av., #1303, Zip Code: 37500-903, Pinheirinho, Itajubá, Brazil.
genesio@unifei.edu.br

Abstract. *Turbulent natural convection of air that happens into inner square cavity with localized heating from horizontal bottom surface has been numerically investigated. Localized heating is simulated by a centrally located heat source on the bottom wall, and two values of the dimensionless heat source length are considered in this present work. Solutions are obtained for several Rayleigh numbers with Prandtl number 0.7. The horizontal top surface is thermally insulated and the vertical surfaces are assumed to be the cold isothermal surfaces whereas the heat source on the bottom wall is isothermally heated. In this study, the Navier-Stokes equations are used considering a two-dimensional and turbulent flow in the unsteady state. The Finite Element Method (FEM) with a Galerkin scheme is considered for solving the conservation equations. The formulation of the conservation equations is carried out for turbulent flow and the turbulence is modeled using Large-Eddy Simulation (LES). The stream function and temperature distributions are determined as functions of thermal and geometrical parameters. The average Nusselt number is shown to increase with an increase in the Rayleigh number as well as in the dimensionless heat source length. The results of this work can be applied to the design of electronic components.*

Keywords: *cavities, finite element method, turbulence, natural convection, LES.*

1. Introduction

Natural convection in enclosures is an area of interest due to its wide application and great importance in engineering. Transient natural convection flows occur in many technological and industrial applications. Therefore, it is important to understand the heat transfer characteristics of natural convection in an enclosure.

Along the years, researchers have looked for more flows with the objective to approximate the real case found in geophysical or industrial means. Then, we can define four basic types of boundary conditions. They are: the natural convection due to a uniformly heated wall (with a temperature or a constant heat flux); the natural convection induced by a local heat source; the natural convection under multiple heat sources with the same strength and type; and the natural convection conjugated with inner heat-generating conductive body or conductive walls. The boundary conditions mentioned previously are based on a single temperature difference between the differentially heated walls. Most of the previous studies have addressed natural convection in enclosures due to either a horizontally or vertically imposed temperature difference. However, departures from this basic situation are often encountered in fields such as electronics cooling. The cooling of electronic components is essential for their reliable performance.

The characteristics of fluid flow and heat transfer under the multiple temperature differences are more complicated and have a practical importance in thermal management and design.

In the present work, a two-dimensional numerical simulation in a cavity is carried out for a turbulent flow. The turbulence study is a complex and challenging assumption. There are few works in literature that deal with natural convection in closed cavities using the turbulence model *LES*. The motivation to accomplish this work relies on the fact that there are a great number of problems in engineering that can use this geometry. One turbulence model is implemented here together with the finite element method.

A large eddy simulation (*LES*) seems a promising approach for the analysis of the high Grashof number turbulence that contains three-dimensional and unsteady characteristics. A direct simulation of turbulence gives us more accurate and precise data than experiments; it is essentially unsuitable for high Grashof number flows because of computational

limitations. It is known that the *LES* enables an accurate prediction of turbulence, but spends much less *CPU* time than the direct simulation.

In literature, a large number of theoretical and experimental investigations are reported on natural convection in enclosures.

Natural convection of air in a two-dimensional rectangular enclosure with localized heating from below and symmetrical cooling from the sides was numerically investigated by Aydin and Yang (2000). Localized heating was simulated by a centrally located heat source on the bottom wall, and four different values of the dimensionless heat source length, $1/5$, $2/5$, $3/5$ and $4/5$ were considered. Solutions were obtained for Rayleigh number values from 10^3 to 10^6 . The average Nusselt number at the heated part of the lower wall, \overline{Nu} , was shown to increase with an increase of the Rayleigh number, Ra , or of the dimensionless heat source length, ϵ .

Peng and Davidson (2001) studied the turbulent natural convection in a closed enclosure whose vertical lateral walls were maintained at different temperatures. Both the Smagorinsk and the dynamic models were applied to the turbulence simulation. Peng and Davidson (2001) modified the Smagorinsk model by adding the buoyancy term to the turbulent viscosity calculation. This model would be called the Smagorinsk model with buoyancy term. The computed results were compared to experimental data and showed a stable thermal stratification under a low turbulence level ($Ra = 1.58 \times 10^9$).

It was performed in the work of Oliveira and Menon (2002), a numerical study of turbulent natural convection in square enclosures. The finite volume method together with *LES* was used. The enclosure lateral surfaces were kept to different isothermal temperatures and the upper and lower surfaces were isolated. The flow was studied for low Rayleigh numbers $Ra = 1.58 \times 10^9$. Three turbulence *LES* models were used.

Ampofo and Karayiannis (2003) conducted an experimental study of low-level turbulence natural convection in an air filled vertical square cavity. The cavity was 0.75 m high \times 1.5 m deep giving rise to a $2D$ flow. The hot and cold walls of the cavity were isothermal at 50 and $10\text{ }^\circ\text{C}$ respectively, that is, a Rayleigh number equals to 1.58×10^9 . The experiments that were realized on Ampofo work and Karayiannis (2003) were conducted with very high accuracy and as such the results formed experimental benchmark data and were useful for validation of computational fluid dynamics codes.

In the present work, turbulent natural convection of air that happens into inner square cavity with localized heating from horizontal bottom surface has been numerically investigated. The objective of the analyses of heat transfer is to investigate the Nusselt number distribution on the vertical walls and heated lower horizontal surface. Another objective is to verify the effect of height variation I of the horizontal heated lower surface on the turbulent flow. Six cases are studied numerically. The Rayleigh number Ra is varied and so is the dimensionless length of the heat source ϵ , where $(1 - \epsilon)/2 \leq x \leq (1 + \epsilon)/2$ and x is the coordinate component in the x direction. For the cases 1, 2 and 3, the dimension ϵ is fixed in $\epsilon = 0.4$ and the Rayleigh numbers Ra is varied ($Ra = 10^7, 10^8, 10^9$). For the cases 1, 2, and 3, it is used a non-structured mesh of finite elements with 5,617 triangle elements with 2,908 nodal points. The other cases also used a non-structured mesh of finite elements with linear triangle elements. In cases 4, 5, and 6, ϵ is fixed in $\epsilon = 0.8$. The cases 1 and 4, 2 and 5 and; 3 and 6 are simulated, respectively, for $Ra = 10^7, 10^8$ and 10^9 . The cases 4, 5, and 6 are simulated with one mesh with 5,828 elements and 3,015 nodes. The turbulence model used in all cases is the Large-Eddy Simulation (*LES*) with the second-order structure-function sub-grid scale model (*F2*). It is adopted a geometry with an aspect ratio $A = H/L = 1.0$. Comparisons are made with experimental data and numerical results found in Tian and Karyiannis (2000), Oliveira and Menon (2002), Lankhorst (1991) and Cesini *et al.* (1999).

2. Problem Description

Figure 1 shows the geometry with the domain Ω . It will be considered a square cavity. The upper horizontal surface S_4 is thermally insulated and the vertical surfaces S_1 and S_3 are assumed to be the cold isothermal surfaces. The bottom horizontal surfaces S_5 and S_6 are also thermally insulated. Localized heating is simulated by a centrally located heat source on the bottom wall, S_2 . The initial condition in Ω is: $T = 0$ with $\psi = \omega = 0$. All physical properties of the fluid are constant except the density in the buoyancy term where it obeys the Boussinesq approximation. It is assumed that the third dimension of the cavities is large enough so that the flow and heat transfer are two-dimensional.

The following hypotheses are employed in the present work: unsteady turbulent regime; incompressible two-dimensional flow; constant fluid physical properties, except the density in the buoyancy terms.

Figure 2 shows one of the meshes used in the numerical simulations of the present work.

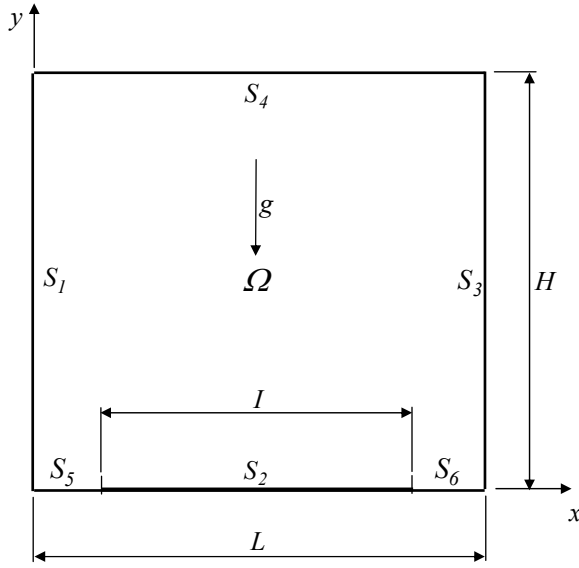


Figure 1: Cavity geometry.

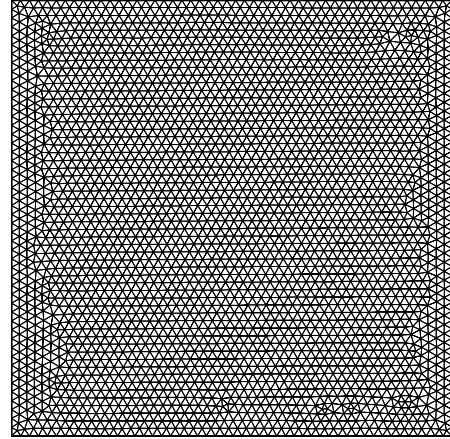


Figure 2: Mesh arrangement for cases 1, 2 and 3.

3. Theory of Sub-Grid Scale Modeling

The governing conservation equations are:

$$\frac{\partial u_i}{\partial x_i} = 0, \quad (1)$$

$$\frac{\partial u_i}{\partial t} + \frac{\partial u_i u_j}{\partial x_j} = -\frac{1}{\rho} \frac{\partial p}{\partial x_i} + \frac{\partial}{\partial x_j} \left\{ \nu \left[\frac{\partial u_i}{\partial x_j} + \frac{\partial u_j}{\partial x_i} \right] \right\} + g\beta(T - T_0)\delta_{2j}, \quad (2)$$

$$\frac{\partial T}{\partial t} + \frac{\partial u_j T}{\partial x_j} = \frac{\partial}{\partial x_j} \left[\alpha \frac{\partial T}{\partial x_j} \right] + S, \quad (3)$$

where x_i are the axial coordinates x and y , u_i are the velocity components, p is the pressure, T is the temperature, ρ is the fluid density, ν is the kinematics viscosity, g is the gravity acceleration, β is the fluid volumetric expansion coefficient, δ_{2j} is the Kronecker delta, α is the thermal diffusivity, and S the source term. The last term in Eq. (2) is the Boussinesq buoyancy term where T_0 is the reference temperature.

In the large eddy simulation (LES), a variable decomposition similar to the one in the Reynolds decomposition is performed, where the quantity φ is split as follows:

$$\varphi = \bar{\varphi} + \varphi', \quad (4)$$

where $\bar{\varphi}$ is the large eddy component and φ' is the small eddy component.

The following filtered conservation equations are shown after applying the filtering operation to Eq. (1) to (3). This is done by using the volume filter function presented in Krajinovic (1998). The density is constant.

$$\frac{\partial \bar{u}_i}{\partial x_i} = 0, \quad (5)$$

$$\frac{\partial \bar{u}_i}{\partial t} + \frac{\partial \bar{u}_i \bar{u}_j}{\partial x_j} = -\frac{1}{\rho} \frac{\partial \bar{p}}{\partial x_i} + \frac{\partial}{\partial x_j} \left\{ \nu \left[\frac{\partial \bar{u}_i}{\partial x_j} + \frac{\partial \bar{u}_j}{\partial x_i} \right] \right\} + g\beta(\bar{T} - T_0)\delta_{2j}, \quad (6)$$

$$\frac{\partial \bar{T}}{\partial t} + \frac{\partial \overline{u_j T}}{\partial x_j} = \frac{\partial}{\partial x_j} \left[\alpha \frac{\partial \bar{T}}{\partial x_j} \right] + S. \quad (7)$$

where x_i are the axial coordinates x and y , u_i are the velocity components, p is the pressure, T is the temperature, ρ is the fluid density, ν is the kinematics viscosity, g is the gravity acceleration, β is the fluid volumetric expansion coefficient, δ_{2j} is the Kronecker delta, α is the thermal diffusivity, and S the source term. The last term in Eq. (2) is the Boussinesq buoyancy term where T_0 is the reference temperature. In Eq. (5) to (7), $\overline{u_i u_j}$ and $\overline{u_j T}$ are the filtered variable products that describe the turbulent momentum transport and the heat transport, respectively, between the large and sub-grid scales. According to Oliveira and Menon (2002), the products $\overline{u_i u_j}$ and $\overline{u_j T}$ are split into other terms by including the Leonard L_{ij} tensor, the Crossing tensor C_{ij} , the Reynolds sub-grid tensor R_{ij} , the Leonard turbulent flux L_θ , the Crossing turbulent flux C_θ and the sub-grid turbulent flux θ . The Crossing and Leonard terms, according to Padilla (2000), can be neglected. After the development shown in Oliveira and Menon (2002), the following conservation equations are obtained:

$$\frac{\partial \bar{u}_i}{\partial x_i} = 0, \quad (8)$$

$$\frac{\partial \bar{u}_i}{\partial t} + \frac{\partial (\bar{u}_i \bar{u}_j)}{\partial x_j} = -\frac{1}{\rho} \frac{\partial \bar{p}}{\partial x_i} + \nu \left(\frac{\partial^2 \bar{u}_i}{\partial x_j \partial x_j} \right) - \frac{\partial \tau_{ij}}{\partial x_i} + g\beta(\bar{T} - T_0)\delta_{2j}, \quad (9)$$

$$\frac{\partial \bar{T}}{\partial t} + \frac{\partial (\bar{u}_j \bar{T})}{\partial x_j} = \frac{\partial}{\partial x_j} \left[\alpha \frac{\partial \bar{T}}{\partial x_j} \right] + \frac{\partial \theta_j}{\partial x_j}, \quad (10)$$

where, Pr is the Prandtl number with $\alpha = \nu/Pr$.

3.1 Sub-grid scale model

According to Silveira Neto (1998), the Reynolds tensor is defined as:

$$\tau_{ij} = -2\nu_T \bar{S}_{ij} - \frac{2}{3} \delta_{ij} \bar{S}_{kk}, \quad \bar{S}_{ij} = \left(\frac{\partial \bar{u}_i}{\partial x_j} + \frac{\partial \bar{u}_j}{\partial x_i} \right), \quad (11)$$

where ν_T is the turbulent kinematics viscosity, δ_{ij} is the Kronecker delta and \bar{S}_{ij} is deformation tensor rate.

Substituting \bar{S}_{ij} in τ_{ij} and having some manipulation, it follows that the momentum and energy equations are:

$$\frac{\partial \bar{u}_i}{\partial t} + \frac{\partial (\bar{u}_i \bar{u}_j)}{\partial x_j} = -\frac{1}{\rho} \frac{\partial \bar{p}}{\partial x_i} + \nu \left(\frac{\partial^2 \bar{u}_i}{\partial x_j \partial x_j} \right) + \frac{\partial}{\partial x_j} \left\{ \nu_T \left[\frac{\partial \bar{u}_i}{\partial x_j} + \frac{\partial \bar{u}_j}{\partial x_i} \right] \right\} + g\beta(\bar{T} - T_0)\delta_{2j}, \quad (12)$$

$$\frac{\partial \bar{T}}{\partial t} + \frac{\partial (\bar{u}_j \bar{T})}{\partial x_j} = \frac{\partial}{\partial x_j} \left[(\alpha + \alpha_T) \frac{\partial \bar{T}}{\partial x_j} \right], \quad \text{with } \alpha_T = \nu_T / Pr_T, \quad \nu_T = c \ell q, \quad \ell = \bar{\Delta} = (\Delta_1 \Delta_2)^{1/2}, \quad (13)$$

where α_T , Pr_T , c , ℓ , q , Δ_1 and Δ_2 are, respectively, the turbulent thermal diffusivity, the turbulent Prandtl number, a dimensionless constant, the scale lengths, the velocity, the filter lengths in x and y directions, respectively.

3.2 The second-order structure-function sub-grid scale model (F2)

The turbulent viscosity (ν_T) and the geometric mean of distances d_i (Δ) are calculated as follows:

$$\nu_T(\bar{x}, \Delta, t) = 0.104 C_k^{-3/2} \Delta \sqrt{\bar{F}_2(\bar{x}, \Delta, t)}, \quad \Delta = \sqrt[N]{\prod_{i=1}^N d_i}, \quad (14)$$

where $C_k = 1.4$ is the Kolmogorov constant (Kolmogorov, 1941), the variable Δ is the geometric mean of distances d_i from neighboring elements to the point where v_T is calculated and $\bar{F}_2(\bar{x}, \Delta, t)$ is the structure function of second order velocities. According to Kolmogorov (1941) law the structure function can be calculated as:

$$\bar{F}_2 = \frac{1}{N} \sum_{i=1}^N \left\{ \left[u_i(\bar{x} + d_i \bar{e}_i, t) - u(\bar{x}, t) \right]^2 + \left[v_i(\bar{x} + d_i \bar{e}_i, t) - v(\bar{x}, t) \right]^2 \right\} \left(\frac{\Delta}{d_i} \right)^{2/3}, \quad (15)$$

where $u_i(\bar{x} + d_i \bar{e}_i, t)$ and $v_i(\bar{x} + d_i \bar{e}_i, t)$ are the velocities at the point “ i ” of the neighboring centroid placed at a distance d_i from the target point, $u(\bar{x}, t)$ and $v(\bar{x}, t)$ are the velocities at this point of the element, N is the number of points from the neighborhood, t is the time and \bar{e}_i the vector on d_i direction.

The turbulent thermal diffusion is estimated from the turbulent kinematics viscosity, by assuming $Pr_T = 0.4$.

4. Initial and boundary conditions

From this section on, the upper bars that mean average values will be omitted. Figure 1 pictures the enclosure on which the initial boundary conditions are as follows: $u(x, y, 0) = 0$, $v(x, y, 0) = 0$, $T(x, y, 0) = 0$ in Ω , $u = v = 0$, $T = T_c = 0$, on S_1 and S_3 , $u = v = 0$, $T = T_h = 1$ on S_2 , $u = v = 0$, $\partial T / \partial y = 0$ on S_4 , S_5 and S_6 . The flow field can be described by the stream function ψ and the vorticity ω distributions given by:

$$u = \partial \psi / \partial y, \quad v = -\partial \psi / \partial x, \quad \omega = (\partial v / \partial x) - (\partial u / \partial y), \quad (16)$$

where u and v are the velocity components in x and y directions, respectively. Hence, the continuity equation given by Eq. (1), is exactly satisfied. Working with dimensionless variables, it is possible to deal with Rayleigh number Ra , Prandtl number Pr and the enclosure aspect ratio A given by:

$$Ra = Pr \left[g \beta (T_h - T_c) H^3 / \nu^2 \right] = 10^7, 10^8 \text{ and } 10^9, \quad Pr = \nu / \alpha = 0.7, \quad A = H / L = 1.0, \quad (17)$$

where T_h and T_c are the surfaces temperatures S_2 and S_1 - S_3 , respectively, H is the characteristic dimension of the cavity.

5. Numerical method

Equations (8) to (10) are solved through the finite element method (FEM) with linear triangular elements using the Galerkin formulation. The local Nusselt number Nu is defined as:

$$Nu = (\partial T / \partial n)_w H / (T_h - T_c), \quad (18)$$

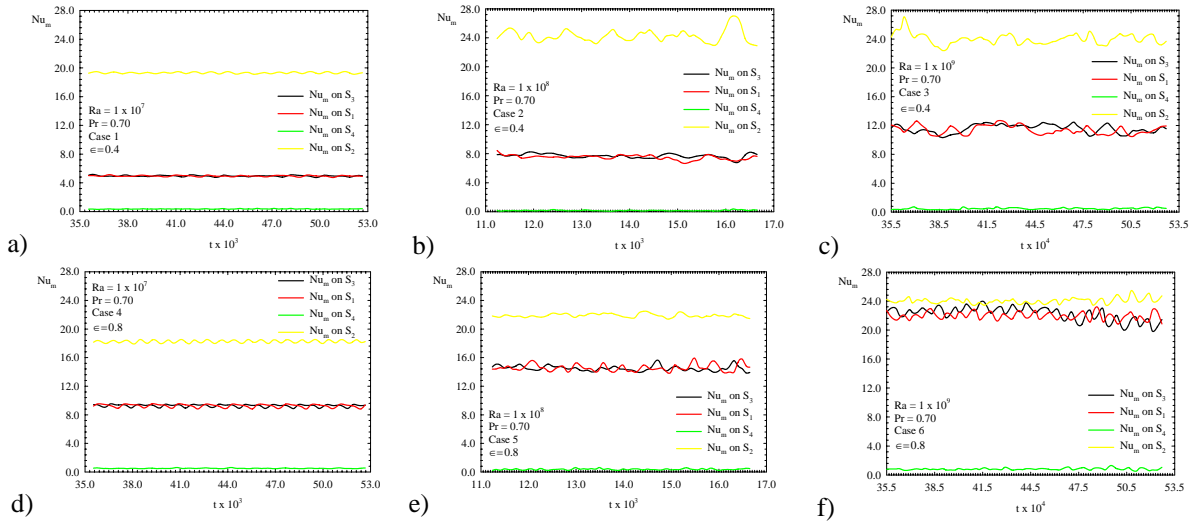
where n is the unit vector normal to the surface or boundary where the local Nusselt number Nu is calculated.

In order to compare the results with the ones found in literature and then to validate the computational code, two cases are taken from Brito *et al.* (2002) and Brito *et al.* (2003). Brito *et al.* (2002) and Brito *et al.* (2003) use the same turbulence model *LES* as the one used in the present work. In the first comparison, the study of the natural turbulent flow in a square enclosure with different temperatures for various Rayleigh numbers is carried out in Brito *et al.* (2002). The second comparison is made in Brito *et al.* (2003) considering a laminar flow in a rectangular enclosure with an internal cylinder. Both results are suitable.

6. Results

The main objective of this study is to analyze the influence of Rayleigh Ra number variation and the length of the heated horizontal lower surface on the flow field. The geometry is chosen in order to simulate the cooling of the air in cavities with electronic components placed on the lower horizontal surface. A Rayleigh number range in a low turbulence flow is: $Ra = 1.0 \times 10^7$, 1.0×10^8 and 1.0×10^9 with $Pr = 0.70$. The geometry parameters used in the six cases mentioned previously are: $H = 1.0$; $L = 1.0$; $T_h = 1$; $T_c = 0$ and $A = H / L = 1.0$. Figure 3 shows the average Nusselt number Nu_m versus time for all six cases. Figure 4 shows the flow fields and the temperature in terms of stream function lines ψ , isotherms T_m and velocity vectors u_i . The time step Δt adopted is $\Delta t = 0.0131 t_0$, $t_0 = H / (g \beta \Delta T H)^{1/2}$, which due to the limitation of the hardware (processor), is three times bigger than the value adopted in Peng and Davidson work

(2001). In Fig. 3, the average time to obtain the average quantities is from 400 to 600 t_0 , $t = (400-600) t_0$. Figure 4 shows the stream function ψ with a line spacing equals to 10 ($\Delta\psi = 10$). For the isotherms, we adopt the same line spacing equals to $\Delta T_m = 0.01$. The stream function ψ is shown for the last interaction, $t = 600 t_0$. The isotherms are calculated at each nodal point considering an average in time, that is, $t = (400-600) t_0$. The same is done to the velocity vectors u_i . Figure 3 shows the average Nusselt numbers Nu_m calculated on surfaces S_1 , S_2 , S_3 and S_4 , versus time t for a time range $t = (400-600) t_0$. Figures 3a, 3b, and 3c, show that the higher the Rayleigh number, the higher the convection in all cavity surfaces studied for fixed values of ϵ . Figures 3d, 3e, and 3f show that heat transfer is higher when the Rayleigh number is increased. In Fig. 3f, the Nu_m values oscillate, due to the effect of the turbulence inside the cavity. The rates of heat transfer are a little larger than those presented in Figures 3a, 3b, and 3c. In Fig. 3, where $Ra = 10^7$, the ϵ increase does not considerably influence the values of Nu_m . Figures 3b and 3e, for $Ra = 10^8$, shows that ϵ increase reduces Nu_m on S_2 . In Figs. 3c and 3f, for $Ra = 10^9$, we observe the same behavior found in Figs. 3b and 3e with $Ra = 10^8$. Then one may conclude that the flow becomes oscillating for $Ra = 10^8$ and $\epsilon = 0.8$, and as it can be seen in Fig. 3f, the heat transfer rates are larger on all the surfaces, including the upper horizontal surface S_4 .



Figures 3: Nu_m versus t on S_1 , S_2 , S_3 and S_4 with $Pr = 0.70$, a-c) $\epsilon = 0.4$, d-f) $\epsilon = 0.8$ for $t = (400-600) t_0$.

Figures 4 shows the effect of Rayleigh number where $10^7 \leq Ra \leq 10^9$ and the effect of the dimensionless length of heat source for $\epsilon = 0.4$ and 0.8 . Due to the symmetrical boundary conditions along the vertical walls, the flow and the temperature fields have a relative symmetry in the middle of the cavity. For the temperature field, it can be observed that this symmetry is better visualized, because the isotherms are obtained through a time average for $t = (400-600) t_0$. These same symmetrical boundary conditions in the vertical direction result in two great fluid areas that symmetrically recirculate. As the flow tends to in the oscillating regime for $Ra = 10^9$, this symmetry is lost.

In Figs. 4a, 4b, and 4c, it is noted that the internal fluid recirculation is more significant as Ra increases. For $Ra = 10^7$, thermal plumes are formed over the hot surface S_2 . The hot fluid which is in the lower region of the cavity moves up due to buoyant forces. During its traveling to the upper part of the cavity, the fluid is cooled on the vertical lateral walls. It can be noted in Fig. 4b that with the Ra increase to $Ra = 10^8$, a region with lower heat transfer is brought about giving rise to a smaller thermal plume. In Fig. 4c, for $Ra = 10^9$, practically all the fluid inside the cavity has a stable average temperature between the maximum and minimum values stated by the boundary conditions. From Figs. 4a, 4b, and 4c, the average velocity vectors picture the fluid behavior in the time range $t = (400-600) t_0$. Figures 4d, 4e, and 4f show the results for $\epsilon = 0.8$ and Ra between $10^7 \leq Ra \leq 10^9$. For Figs. 4d, 4e, and 4f, where $\epsilon = 0.8$, the increase of the heated surface length S_2 makes the heat transfer increase in all surfaces. The surface S_2 has the reduction of the Nu_m value calculated for the range 400 to 600 t_0 with $Ra = 10^7$. For the isotherms, Figs. 4e and 4f show few differences. The streamlines, in Figs. 4d, 4e, and 4f show two big fluid regions that move in opposite directions.

7. Discussion

In this investigation, the results of a numerical study of buoyancy-induced flow and heat transfer in a two-dimensional square enclosure with localized heating from below and symmetrical cooling from the sides are presented. The main parameters of interest are Rayleigh number Ra and the dimensionless heat source length ϵ .

One kind of sub-grid scale model is used: large-eddy simulation (LES) with the second-order structure-function sub-grid scale model (F2) (more details in Silveira Neto, 1998). The conservation equations are discretized by the Galerkin finite element method with linear triangular elements.

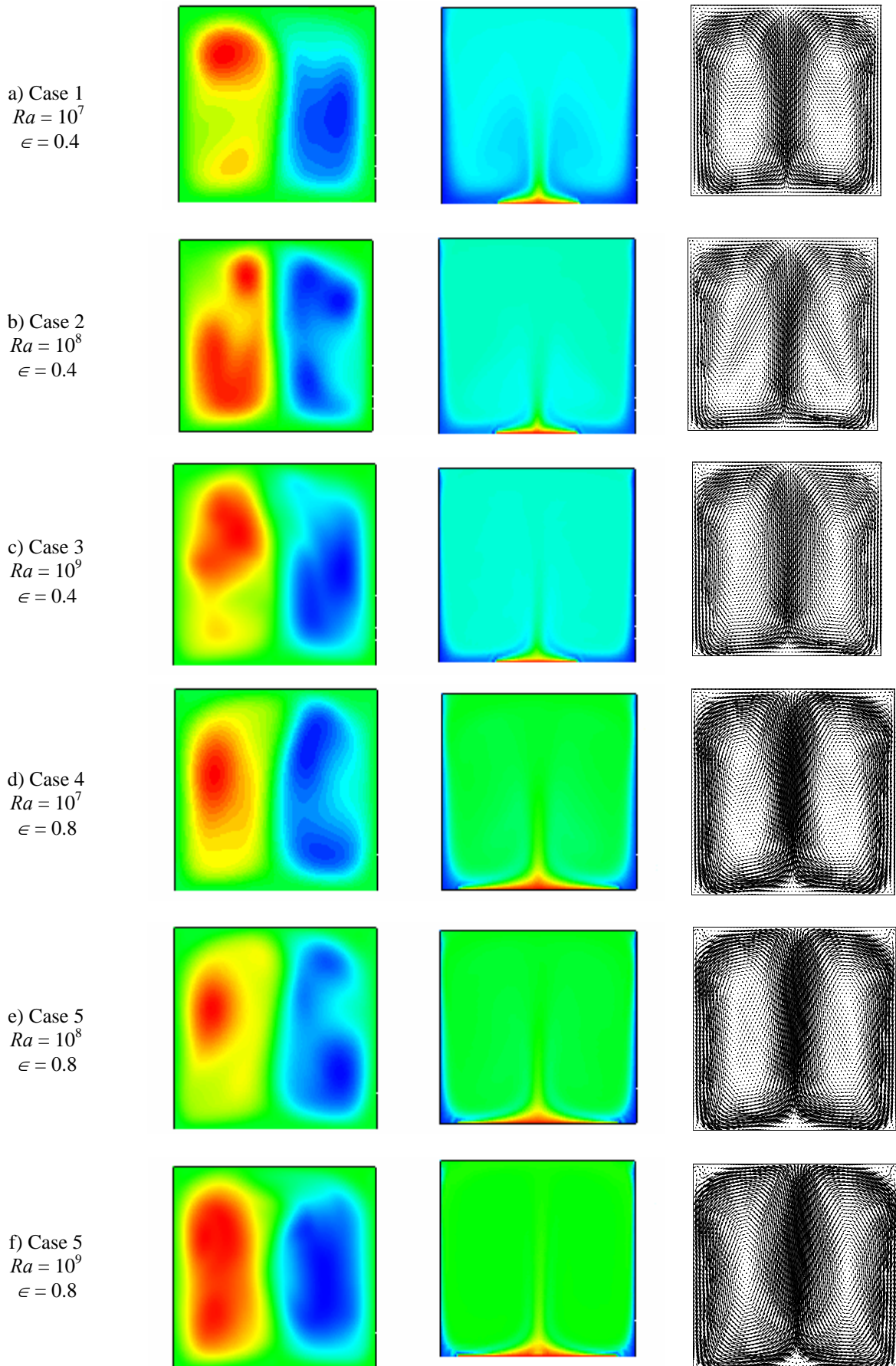


Figure 6: Streamfunction ψ for $t = 600 t_0$ ($\Delta\psi = 10$), average temperature, T_m ($\Delta T_m = 0.01$) for $t = (400-600) t_0$ and velocity vectors for $t = (400-600) t_0$ and $Pr = 0.7$.

Two cases are used for validation of the computational domain of the present work. In Brito *et al.* (2002) and Brito *et al.* (2003), the same turbulence model *LES*, together with the finite element method, is used in the present work.

It is observed that increasing Ra , the rate of heat transfer also increased, as expected. For a fixed value of Ra , the ϵ increase also increases the heat transfer. For $Ra = 10^9$ and $\epsilon = 0.8$, although the flow is considered two-dimensional, it is noticed that the flow becomes oscillating in time which is a typical characteristic of a flow in transition to turbulence. The average temperature T_m and velocity vectors u_i distributions are presented for Rayleigh number $10^7 \leq Ra \leq 10^9$ and Prandtl number $Pr = 0.70$ for $t = (400-600) t_0$. The results of streamfunction ψ distributions are presented for $t = 600 t_0$.

8. Acknowledgements

The authors thank the financial support from CNPq and CAPES without which this work would be impossible.

9. References

- Ampofo, F. and Karayiannis, T.G., 2003, "Experimental Benchmark Data for Turbulent Natural Convection in an Air Filled Square Cavity", *International Journal of Heat and Mass Transfer*, Vol. 46, pp 3551-3572.
- Aydin, O. and Yang, W.-J., 2000, "Natural Convection in Enclosures with Localized Heating from Below and Symmetrical Cooling from Sides", *International Journal of Numerical Methods for Heat & Fluid Flow*, Vol. 10, n° 5, pp 518-529.
- Brito, R. F., Guimarães, P. M., Silveira-Neto, A., Oliveira, M. and Menon, G. J., 2003, "Turbulent Natural Convection in a Rectangular Enclosure using Large Eddy Simulation", *Proceedings of the 17th International Congress of Mechanical Engineering – COBEM – São Paulo – Brazil*, pp 1-10.
- Brito, R. F., Silveira-Neto, A., Oliveira, M. and Menon, G. J., 2002, "Convecção Natural Turbulenta em Cavidade Retangular com um Cilindro Interno", *Proceedings of the first South-American Congress on Computational Mechanics - MECOM - III Brazilian Congress on Computational Mechanics - VII Argentine Congress on Computational Mechanics - Santa Fe-Paraná – Argentina*, pp 620-633.
- Cesini, G., Paroncini, M., Cortella G. and Manzan, M., 1999, "Natural Convection from a Horizontal Cylinder in a Rectangular Cavity", *International Journal of Heat and Mass Transfer*, Vol. 42, pp 1801-1811.
- Kolmogorov, A. N., 1941, "The Local Structure of Turbulence in Incompressible Viscous Fluid for Very Large Reynolds Numbers", *Dokl. Akad. Nauk SSSR*, Vol. 30, pp 301-305.
- Krajnovic, S., 1998, *Large-Eddy Simulation of the Flow Around a Surface Mounted Single Cube in a Channel*, Ms. C. Thesis, Chalmers University of Technology, Goteborg, Sweden.
- Lankhorst, A. M., 1991, *Laminar and Turbulent Natural Convection in Cavities – Numerical Modelling and Experimental Validation*, Ph. D. Thesis, Technology University of Delft, The Netherlands.
- Oliveira, M. and Menon, G. J., 2002, "Simulação de Grandes Escalas Utilizada para Convecção Natural Turbulenta em Cavidades", *Proceedings of the 9th Congresso Brasileiro de Engenharia e Ciências Térmicas - ENCIT-2002, Caxambu - Brazil*, CD ROM, pp 1-11.
- Padilla, E. L. M., 2000, *Simulação Numérica de Grandes Escalas com Modelagem Dinâmica, Aplicada à Convecção Mista*, Ms. C. Thesis, DEEME-UFU, Uberlândia, Brazil.
- Peng, S. H. and Davidson, L., 2001, "Large-Eddy Simulation for Turbulent Buoyant Flow in a Confined Cavity", *Int. J. Heat and Fluid Flow*, Vol. 22, pp 323-331.
- Silveira-Neto, A., 1998, "Simulação de Grandes Escalas de Escoamentos Turbulentos", *Proceedings of the I Escola de Primavera de Transição e Turbulência*, Vol.1, Rio de Janeiro, Brazil, pp 157-190.
- Tian, Y. S. and Karayiannis, T. G., 2000a, "Low Turbulence Natural Convection in an Air Filled Square Cavity Part I: The Thermal and Fluid Flow Fields", *Int. J. Heat and Mass Transfer*, Vol. 43, pp 849-866.
- Tian, Y. S. and Karayiannis, T. G., 2000b, "Low Turbulence Natural Convection in an Air Filled Square Cavity - Part II: the Turbulence Quantities", *Int. J. Heat and Mass Transfer*, Vol. 43, pp 867-884.

10. Responsibility notice

The authors are the only responsible for the printed material included in this paper.